

A CLASS OF IMPROVED PULSES GENERATED BY NYQUIST FILTERS

Nicolae Dumitru ALEXANDRU

*Gh. Asachi” Technical University of Iași
Department of Telecommunications
Bd. Carol I no 11, 700506 - Iași, ROMANIA
nalex@etc.tuiasi.ro*

Maria Liliana ALEXANDRU

*“G. Ibrăileanu” Highschool Iași
l_alex21@yahoo.com*

Ligia Alexandra ONOFREI

*“Ștefan cel Mare” University of Suceava
str. Universității nr.13, RO-720225 Suceava
onofreial@eed.usv.ro*

Abstract: *A novel class of ISI-free pulses is presented and investigated. We propose and investigate a class of new Nyquist pulses that shows comparable or better ISI performance in the presence of sampling errors, as compared with some recently proposed pulses.*

Keywords: *intersymbol interference, Nyquist filter, error probability.*

1. Introduction

Recently, improved Nyquist pulses that show smaller maximum distortion, more open receiver eye and a smaller symbol error rate in the presence of symbol timing error were reported [2,3 and 4]. They are defined by

$$S_i(f) = \begin{cases} 1, & |f| \leq B(1-\alpha) \\ G(|f| - B(1-\alpha)), & B(1-\alpha) \leq |f| \leq B \\ 1 - G(B(1+\alpha) - |f|), & B < |f| \leq B(1+\alpha) \\ 0, & B(1+\alpha) < |f| \end{cases} \quad (1)$$

where $G(f)$ is a function satisfying $G(0)=1$. In [2,3 and 4] $G(f)$ was chosen to have a particular shape in the frequency interval $B(1-\alpha) \leq |f| \leq B$ in order to transfer some energy to the high frequency spectral range. This results in a pulse that decays asymptotically as t^{-2} as compared with t^{-3} for the RC pulse, but with the advantage that the eye diagram is more open and, as a consequence, a better bit error rate is obtained.

Two recent contributions showed that improved Nyquist pulses could be obtained with the *flipped- $G(f)$* technique, e.g. *flipped-exponential* [2] and *flipped-hyperbolic secant* or *flipped-inverse hyperbolic secant* [3].

The envelope of the impulse response decays as t^{-2} or t^{-3} at best, since the functions and their flipped counterparts are continuous at $f_n = 1$.

The first derivative of the *flipped-hyperbolic secant* is continuous at $f_n = 1$, which accounts for its steeper decay. The *flipped-exponential* technique uses $G(f) = e^f$ and $\beta = \ln 2 / (\alpha B)$, while

in [3] $G(f) = \operatorname{sech}(f)$ and $\beta = \gamma = \ln(\sqrt{3} + 2) / (\alpha B)$ or $X(f) = 1 - \frac{1}{2\alpha B \gamma} \operatorname{arc\,sec\,h}(f)$ with $\beta = \frac{1}{2\alpha B}$.

2. A class of new Nyquist pulses

We propose a class of new Nyquist pulses with piece-wise characteristics, that are defined for positive frequencies and even i as

$$S_i(f) = \begin{cases} 1, & |f| \leq B(1-\alpha) \\ G(|f| - B(1-\alpha)), & B(1-\alpha) \leq |f| \leq B(1-b) \\ H_i(|f| - B), & B(1-b) \leq |f| \leq B \\ 1 - H_i(|f| - B), & B < |f| \leq B(1+b) \\ 1 - G(B(1+\alpha) - |f|), & B(1+b) < |f| \leq B(1+\alpha) \\ 0, & B(1+\alpha) < |f| \end{cases} \quad (2)$$

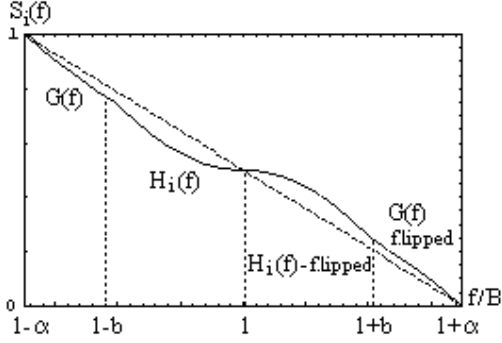


Figure 1 Proposed filter characteristic

The Nyquist filter characteristic is obtained from combining two types of characteristics with odd-symmetry. Here $G(f)$ is the *flipped-exponential* characteristic proposed in [2] and $H_i(f)$ is the family of parabolic, cubic and quartic ramps proposed in [5].

$$G(f) = e^f$$

$$H_i(f) = -(-1)^i \frac{(f-B)^i}{B^i b^i} \left(e^{\frac{\ln 2(b-\alpha)}{\alpha}} - \frac{1}{2} \right) + \frac{1}{2} \quad (2)$$

For i odd they show odd symmetry around B and their definition is

$$S_i(f) = \begin{cases} 1, & |f| \leq B(1-\alpha) \\ G(f), & B(1-\alpha) \leq |f| \leq B(1+b) \\ H_i(f), & B(1-b) \leq |f| \leq B(1+b) \\ G(f) - \text{flipped}, & B(1+b) \leq |f| \leq B(1+\alpha) \\ 0, & B(1+\alpha) < |f| \end{cases} \quad (3)$$

For i even, the vestigial symmetry is obtained by choosing $H_i(f)$ for the frequency interval $B(1-\alpha) \leq f \leq B$ and $1 - H_i(f)$ for $B \leq f \leq B(1+\alpha)$.

The expressions were derived imposing continuity conditions at $f = B(1-b)$ and $f = B(1+b)$ and a value of 0.5 at $f = B$.

This technique will be denoted in the sequel as *double-ramp flipped- $G(f)$* and is illustrated in Fig.1.

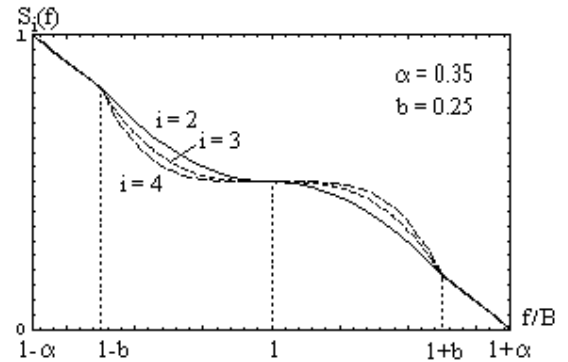


Figure 2 A class of proposed frequency characteristics (positive frequencies)

Figure 2 illustrates this class of new Nyquist filter characteristics for $i = 2, 3, \text{ and } 4$.

Since they are more concave than the FE pulse, a decrease of the first side lobe in time domain is to be expected, as shown in Fig.3, where a time-scaled replica of pulses is represented for $\alpha = 0.25$. The impulse responses $s_i(t)$ are given in the Appendix A.

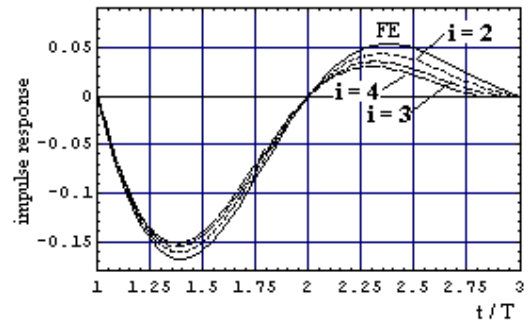


Figure 3 Impulse responses $\alpha = 0.25$

Their behavior around $t/T = 3, 4, \dots$ is more flat, which accounts for their better properties regarding the error probability when sampled with a small time offset.

A look at Fig.3 that further illustrates the decay of impulse responses reveals that the new pulse defined by (1) and (2) with $i = 2$ follows closely the FE pulse.

Regarding the other pulses ($i = 3$ and 4), though the decrease of the first side lobe is more

3. Conclusions

A new class of Nyquist pulses that show reduced maximum distortion, a more open receiver eye and decreased symbol error probability in the presence of timing error as compared with the FE pulse [2] with the same roll-off factor was introduced. Its transmission properties were thoroughly investigated and show that the pulses have practical importance.

Table 1: ISI error probability of several Nyquist pulses for $N=2^{10}$ interfering symbols and SNR = 15 dB

P_e	B=1		$t/T_B = \pm 0.05$	$t/T_B = \pm 0.1$	$t/T_B = \pm 0.2$	$t/T_B = \pm 0.3$
	α	b				
FE	0.25		$5.81166 \cdot 10^{-8}$	$1.29804 \cdot 10^{-6}$	$3.56785 \cdot 10^{-4}$	$1.45241 \cdot 10^{-2}$
	0.35		$3.92526 \cdot 10^{-8}$	$5.40211 \cdot 10^{-7}$	$1.01287 \cdot 10^{-4}$	$5.88798 \cdot 10^{-3}$
	0.5		$2.41342 \cdot 10^{-8}$	$1.85795 \cdot 10^{-7}$	$2.08778 \cdot 10^{-5}$	$1.57719 \cdot 10^{-3}$
c2	0.25	0.24	$5.35869 \cdot 10^{-8}$	$1.1125 \cdot 10^{-6}$	$2.95331 \cdot 10^{-4}$	$1.25179 \cdot 10^{-2}$
	0.35	0.34	$3.59187 \cdot 10^{-8}$	$4.69738 \cdot 10^{-7}$	$8.91204 \cdot 10^{-5}$	$5.17815 \cdot 10^{-3}$
	0.5	0.49	$2.22421 \cdot 10^{-8}$	$1.69435 \cdot 10^{-7}$	$2.27295 \cdot 10^{-5}$	$1.8209 \cdot 10^{-3}$
c3	0.25	0.24	$5.14109 \cdot 10^{-8}$	$1.05201 \cdot 10^{-6}$	$2.82402 \cdot 10^{-4}$	$1.1828 \cdot 10^{-2}$
	0.35	0.34	$3.46657 \cdot 10^{-8}$	$4.65864 \cdot 10^{-7}$	$9.6416 \cdot 10^{-5}$	$5.39191 \cdot 10^{-3}$
	0.5	0.49	$2.19888 \cdot 10^{-8}$	$1.77572 \cdot 10^{-7}$	$3.03206 \cdot 10^{-5}$	$2.64191 \cdot 10^{-3}$
c4	0.25	0.24	$5.06443 \cdot 10^{-8}$	$1.04682 \cdot 10^{-6}$	$2.87321 \cdot 10^{-4}$	$1.17539 \cdot 10^{-2}$
	0.35	0.34	$3.44572 \cdot 10^{-8}$	$4.8368 \cdot 10^{-7}$	$1.08168 \cdot 10^{-4}$	$5.83255 \cdot 10^{-3}$
	0.5	0.49	$2.23808 \cdot 10^{-8}$	$1.91963 \cdot 10^{-7}$	$3.92872 \cdot 10^{-4}$	$3.54274 \cdot 10^{-3}$

significant, the side lobes are significantly larger, which results in increased ISI. The behaviour is similar to that of FE pulse where increasing α results in decreased error probability.

3. Error probability

When the receiver eye is sampled off center, as in practical receivers, timing error results in an increase of the average symbol error probability [2, 3, 14].

This is calculated using the method of [13] for all proposed pulses and illustrated in Table I, together with those for FE pulse.

4. References

- [1] Nyquist, H. (1928) "Certain topics in telegraph transmission theory" *AIEE Trans.*, vol. 47, pp. 617–644.
- [2] Beaulieu, N. C., Tan, C. C., and Damen, M. O. (2001) "A "better than" Nyquist pulse," *IEEE Commun. Lett.*, vol. 5, pp. 367–368, Sept..
- [3] Assalini, A. and Tonello, A. M. (2004) "Improved Nyquist pulses," *IEEE Communications Letters*, vol. 8, pp. 87 - 89, February.
- [4] Beaulieu N. C. and Damen, M. O., (2004) "Parametric construction of Nyquist-I pulses," *IEEE Trans. Communications*, vol. COM-52, pp. 2134 - 2142, December.

- [5] Alexandru, N.D. and Onofrei, L.A. (2006), "A Novel Class of Improved Nyquist Pulses", ECUMICT 2006, Ghent, Belgium.
- [6] Xia, X.-G. (1997) "A family of pulse-shaping filters with ISI-free matched and unmatched filter properties," *IEEE Trans. Commun.*, vol. 45, pp. 1157–1158, Oct.
- [7] Demechai, T. (1998) "Pulse-shaping filters with ISI-free matched and unmatched filter properties," *IEEE Trans. Commun.*, vol. 46, p. 992, Aug..
- [8] Tan, C. C. and Beaulieu, N. C. (2004) "Transmission properties of conjugate-root pulses," *IEEE Trans. Commun.*, vol. 52, pp. 553–558, Apr.
- [9] Franks, L. E. (1968) "Further results on Nyquist's problem in pulse transmission," *IEEE Trans. Commun. Technol.*, vol. COM-16, pp. 337–340, Apr.

- [10] Kisel A. V., (1999) "An extension of pulse shaping filters theory," *IEEE Trans. Commun.*, vol. 47, pp. 645–647, May.
- [11] Andrisano, O. and Chiani, M. (1994) "The first Nyquist criterion applied to coherent receiver design for generalized MSK signals," *IEEE Trans. Commun.*, vol. 42, Feb./Mar./Apr.
- [12] Sayar, B. and Pasupathy, S. (1987). "Nyquist 3 pulse shaping in continuous phase modulation," *IEEE Trans. Commun.*, vol. COM-35, pp. 57–67, Jan.
- [13] Beaulieu, N. C. (1991) "The evaluation of error probabilities for intersymbol and cochannel interference," *IEEE Trans. Commun.*, vol. 31, pp.1740–1749, Dec.
- [14] Hill Jr., F. S. (1977) "A unified approach to pulse design in data transmission," *IEEE Trans. Commun.*, vol. COM-25, pp. 346–354, Mar..

Appendix

$$\begin{aligned}
c_2(t) = & \frac{1}{8} \left\{ -\frac{8 \sin((\alpha-1)B\pi)}{\pi} + \right. \\
& \frac{4aB \left(\cos((\alpha-1)B\pi) \log(4) + 2aB\pi \sin((\alpha-1)B\pi) - 2^{\frac{b}{\alpha}} (\cos((b-1)B\pi) \log(2) + \alpha B\pi \sin((b-1)B\pi)) \right)}{\alpha^2 B^2 \pi^2 t^2 + \log(2)^2} + \\
& \frac{1}{b^2 B^2 \pi^3 t^3} \left(\left(\left(\left(1 - 2^{\frac{b}{\alpha}} \right) (\sin(B\pi) + \sin((-1+b)B\pi)) + \right. \right. \right. \\
& \left. \left. \left. bB\pi \left(\left(2^{\frac{b}{\alpha}} - 1 \right) \cos((b-1)B\pi) + \frac{1}{2} bB\pi \left(\sin(B\pi) + 2^{\frac{b}{\alpha}} \sin((b-1)B\pi) \right) \right) \right) \right) \right) + \\
& \frac{1}{b^2 B^2 \pi^3 t^3} \left(\left(\left(\left(2^{\frac{b}{\alpha}} - 1 \right) (-\sin(B\pi) + \sin((1+b)B\pi)) + \right. \right. \right. \\
& \left. \left. \left. bB\pi \left(\left(1 - 2^{\frac{b}{\alpha}} \right) \cos((1+b)B\pi) - \frac{1}{2} bB\pi \left(\sin(B\pi) + \left(2^{\frac{b}{\alpha}} - 2 \right) \sin((1+b)B\pi) \right) \right) \right) \right) \right) + \\
& 4 \left(\frac{2(\sin((1+\alpha)B\pi) - \sin((1+b)B\pi))}{\pi t} + \right. \\
& \left. \frac{aB \left(-2 \cos((1+\alpha)B\pi) \log(2) - 2\alpha B\pi \sin((1+\alpha)B\pi) + 2^{\frac{b}{\alpha}} (\cos((1+b)B\pi) \log(2) + \alpha B\pi \sin((1+b)B\pi)) \right)}{\alpha^2 B^2 \pi^2 t^2 + \log(2)^2} \right) \left. \right\}
\end{aligned}$$

$$\begin{aligned}
c_3(t) = & \frac{1}{16B^3} \left\{ \cos((-1+b)B\pi t) \left[\frac{16 \left(3 - 3 \cdot 2^{\frac{b}{\alpha}} \right)}{b^3 \pi^4 t^4} + \frac{24 \left(2^{\frac{b}{\alpha}} - 1 \right) B^2}{b \pi^2 t^2} - \frac{2^{3+\frac{b}{\alpha}} \alpha B^4 \log(2)}{\alpha^2 B^2 \pi^2 t^2 + \log(2)^2} \right] + \right. \\
& \frac{1}{b^3 \pi^4 t^4 (\alpha^2 B^2 \pi^2 t^2 + \log(2)^2)} \left\{ 16 \left[\cos((1+b)B\pi t) \left(-3 \left(-1 + 2^{\frac{b}{\alpha}} \right) \alpha^2 B^2 \pi^2 t^2 \left(\frac{b^2 B^2 \pi^2 t^2}{2} - 1 \right) + \right. \right. \\
& \left. \left. 2^{-1+\frac{b}{\alpha}} \alpha b^3 B^4 \pi^4 t^4 \log(2) - 3 \left(-1 + 2^{\frac{b}{\alpha}} \right) \left(-1 + \alpha^2 B^2 \pi^2 t^2 \right) \log(2)^2 \right] + \right. \\
& \left. bB\pi t \left(2b^2 B^2 \pi^2 t^2 \cos(\alpha B\pi t) \log(2)^2 \sin(B\pi t) + \alpha b^2 B^3 \pi^3 t^3 \log(4) \sin(B\pi t) \sin(\alpha B\pi t) + \right. \right. \\
& \left. \left. \left(3 \left(2^{\frac{b}{\alpha}} - 1 \right) \alpha^2 B^2 \pi^2 t^2 + \left(2^{\frac{b}{\alpha}} \left(3 - \frac{b^2 B^2 \pi^2 t^2}{2} \right) - 3 \right) \log(2)^2 \right) \left(\sin((b+1)B\pi t) - \sin((b-1)B\pi t) \right) \right] \right\} \left. \right\}
\end{aligned}$$

$$\begin{aligned}
c_4(t) = & \frac{1}{8} \left\{ -\frac{8 \sin((\alpha-1)B\pi t)}{\pi t} + \frac{1}{\alpha^2 B^2 \pi^2 t^2 + \log(2)^2} \left[4\alpha B \left(\cos((\alpha-1)B\pi t) \log(4) + 2\alpha B\pi t \sin((\alpha-1)B\pi t) - \right. \right. \right. \\
& \left. \left. 2^{\frac{b}{\alpha}} (\cos((b-1)B\pi t) \log(2) + \alpha B\pi t \sin((b-1)B\pi t)) \right] \right\} + \\
& \frac{1}{b^4 B^4 \pi^5 t^5} \left\{ 32 \left[3 \left(2^{\frac{b}{\alpha}} - 1 \right) (\sin(B\pi t) + \sin((b-1)B\pi t)) + \right. \right. \\
& \left. \left. bB\pi t \left(\left(2^{\frac{b}{\alpha}} - 1 \right) \left(-\frac{b^2 B^2 \pi^2 t^2}{2} - 3 \right) \cos((b-1)B\pi t) + \right. \right. \\
& \left. \left. \frac{1}{8} b^3 B^3 \pi^3 t^3 \sin(B\pi t) + \frac{1}{2} bB\pi t \left(3 + 2^{\frac{b}{\alpha}} \left(\frac{b^2 B^2 \pi^2 t^2}{4} - 3 \right) \right) \sin((b-1)B\pi t) \right] \right\} + \\
& \frac{1}{b^4 B^4 \pi^5 t^5} \left\{ 32 \left[-\left(-1 + 2^{\frac{b}{\alpha}} \right) bB\pi t \left(\frac{b^2 B^2 \pi^2 t^2}{2} - 3 \right) \cos((1+b)B\pi t) + \left(3 \cdot 2^{\frac{b}{\alpha}} - 3 - \frac{b^4 B^4 \pi^4 t^4}{8} \right) \sin(B\pi t) + \right. \right. \\
& \left. \left(3 - 3 \left(2^{\frac{b}{\alpha}} \right) + \frac{3}{2} \left(2^{\frac{b}{\alpha}} - 1 \right) b^2 B^2 \pi^2 t^2 - \frac{1}{8} \left(2^{\frac{b}{\alpha}} - 2 \right) b^4 B^4 \pi^4 t^4 \right) \sin((1+b)B\pi t) \right] \right\} + \\
& 4 \left\{ \frac{2(\sin((1+\alpha)B\pi t) - \sin((1+b)B\pi t))}{\pi t} + \frac{1}{\alpha^2 B^2 \pi^2 t^2 + \log(2)^2} \left[\alpha B \left(-\cos((1+\alpha)B\pi t) \log(4) - \right. \right. \right. \\
& \left. \left. 2\alpha B\pi t \sin((1+\alpha)B\pi t) + \right. \right. \\
& \left. \left. 2^{\frac{b}{\alpha}} (\cos((1+b)B\pi t) \log(2) + \alpha B\pi t \sin((1+b)B\pi t)) \right] \right\}
\end{aligned}$$